Freeform Surface Filtering Using the Lifting Wavelet Transform

Hussein S. Abdul-Rahman[1], Xiangqian (Jane) Jiang*[1] and Paul J. Scott[1]

h.abdul-rahman@hud.ac.uk, *corresponding author: x.jiang@hud.ac.uk , p.j.scott@hud.ac.uk

[1]*EPSRC Centre for Innovative Manufacturing in Advanced Metrology, Centre for Precision Technologies, School of Computing and Engineering, University of Huddersfield, Huddersfield HD1 3DH, UK.*

***Abstract*-Texture measurement for simple geometric surfaces is well established. Many surface filtration techniques using Fourier, Gaussian, wavelets … etc, have been proposed over the past decades. These filtration techniques cannot be applied to today's complex freeform surfaces, which have non-Euclidean geometries in nature, without distortion of the results. Introducing the lifting scheme open the opportunity to extend the wavelet analysis to include irregular complex surface geometries. Using the second generation wavelets and the lifting scheme, a method of texture filtration for freeform surface data is proposed in this paper. Results and discussion of the application of this method to simulated and measured data are presented.**

***Index Terms*—freeform surfaces; irregular wavelets; lifting scheme; surface metrology; wavelet analysis; wavelets on triangular meshes.**

I- Introduction

Over many years, the theory of measuring and characterising ordinary simple surfaces such as planes, spheres and cylinders has been developed [1-5]. Indeed, many research papers and industrial standards have been published to describe the measurement and characterisation of such surfaces [3-9]. However, with the development of science and technology, more and more complex surfaces are being produced which, unlike the conventional surfaces, have no axes of rotation and no translational symmetry and could have any shape or design; such complex surfaces are called freeform surfaces.

Characterisation and parameterisation of surface texture on such freeform geometries is very challenging and requires re-thinking each step of characterising the texture on simple surfaces. Traditionally, the characterisation and parameterisation of surface texture is carried out using the four major steps namely; surface sampling and representation, decomposition and filtration, texture representation and mapping and finally characterisation and parameterisation as shown in Fig. 1.

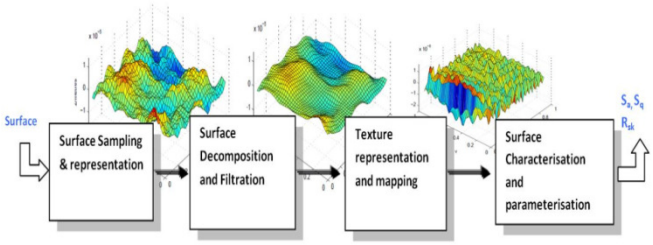

Fig. 1: Texture characterisation and parameterisation

Moving from simple geometries to complex freeform geometries, many of the traditional techniques used to perform any of the tasks shown in Fig. 1 start to fail. Therefore, new theories and tools that can cope with the new emerging surfaces are required.

Surface decomposition and filtration is an essential step of the texture characterisation system. During the last decade, decomposition and filtration techniques for simple surfaces have been comprehensively investigated and many algorithms based on Fourier, Gaussian, Spline and wavelet techniques were proposed and became the industrial filtration standards for such surfaces [6-10]. Unfortunately, all of these techniques are designed to decompose and filter Euclidean surfaces, so most of these techniques fail to filter freeform non-Euclidean surfaces.

Very recently, our research group have proposed a new filtration technique for freeform surfaces, represented by triangular meshes, based on solving the diffusion equation formulated by using the Laplace-Beltrami operator on that surface [11].

In this paper, we provide an initial investigation of applying the lifting wavelet for freeform surface filtration. The power of this filtration technique is that it's capable to filter any type or shape of surfaces. We investigate different methods of building the lifting scheme and the results are discussed and presented.

This paper is organised as follows; section 2 discusses different techniques to represent a freeform surfaces, section 3 gives a brief introduction about the lifting scheme and the second generation wavelets. A brief review of wavelets and multi-resolution analysis on surface is shown in section 4. Section 5 details the proposed lifting algorithm on freeform

surfaces and the results of the algorithm is shown in section 6. Finally, the conclusions and future work is discussed in section 7.

II- REPRESENTING FREEFORM SURFACES

Traditionally, surfaces are represented as height values over plane. This type of representation is only valid for simple Euclidean surfaces. This type of representation enables researcher to successfully apply different processing techniques, such as Fourier analysis, wavelet decomposition and Gaussian filters, to analyse surfaces' data. Freeform surfaces cannot be represented using the traditional method and new method of representing freeform surfaces is required.

Fortunately, there are a number of freeform surface representation techniques found in the field of computer graphics, computer design and many other fields. These techniques can be roughly classified into; discrete method, continuous methods. A survey of surface representation techniques can be found in [12].

The discrete representation consists mainly of two major types; point clouds and polygon surface meshes. Point clouds is a very primitive way of representing a surface, it is only store the surface as a number of (x,y,z) coordinates and no geometrical properties can be obtained from this type of presentation. Surface meshes, on the other hand, are widely used to represent surfaces of different topological types. Geometrical approximation and surface information can be derived from the surface mesh.

Continuous representation methods attempt to describe the freeform surface using an equation or a set of equations. NURBS, B-SPLINE are the two major types of the continuous methods. Describing a freeform surface using mathematical equations is not trivial and requires fitting algorithms, and also they require that data to be represented by meshes.

Because of the reasons that polygon surface meshes is easier to implement and they can easily represent any freeform surface and also because they have been used to represent surfaces in many different applications and geometrical approximation could be extracted from them, polygon surface meshes are adopted to represent the freeform surfaces in this paper and in particular, the triangular surface meshes.

A triangular mesh can be simply defined as a collection of vertices (points), edges and faces that define the shape or a surface of a 3D object. Three major types of meshes according to the distribution of the vertices, edges and faces among the entire surface can be distinguished; regular, semi-regular and irregular meshes as shown in Fig. 2 [13].

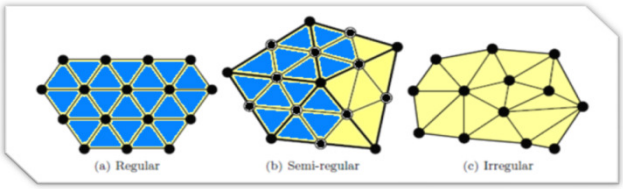

Fig. 2: Different types of triangular mesh: (a) regular, (b) semi-regular and (c) irregular

Regular Meshes is a type of mesh where its vertices are regularly distributed among the entire surface, all the faces have almost the same area and finally all vertices have the same number of edges. Semi-regular mesh is a mesh that is considered to be regular on local areas but not on the entire surface. On the other hand, irregular mesh is that mesh which does not possess any of the above properties, the area of each face (triangle) is different to the other, and also the number of edges per vertex is varying [13].

Most of regular and semi-regular types of meshes can be found in computer graphics and computer generated surfaces and object and it is not very common to be found in actual measured surfaces. Irregular type meshes are more realistic and suitable from surface texture point of view than the other two types, therefore we focus to filter freeform surfaces represented by irregular meshes as will be shown in this paper.

III- SECOND GENERATION WAVELET AND THE LIFTING SCHEME

Wavelets are very powerful tool for representing and decomposing general function, curves, surfaces or any type of data sets into their basic components. They enjoy a very widespread use in many different areas and applications such as signal processing, image processing, image compression, computer graphics, surface filtration and many others. The power of wavelets derives from representing the input data sets into time-scale and different levels of resolution.

Traditionally, wavelets analysis was defined as translation and dilation of one particular function called the mother wavelet. This translation and dilation was carried out by convolving the input data with a series of filter banks. This type of wavelet transform was called the first generation wavelets.

First generation wavelets can only be applied to regular data such as regular sampled signals, images and Euclidean surfaces. However, many applications have irregular data sets and therefore new generation of wavelets were required. In 1995, Swelden proposed the lifting scheme as a new generation of wavelets, which he referred as the second generation wavelets. The lifting scheme generalises the first generation and could be applied for both regular and irregular data sets [14-17].

The lifting scheme allows the construction of the filter banks entirely in the spatial domain and eliminates the need of Fourier or convolution operation which limits the first generation to only regular data sets. Instead of explicitly

designing and specifying the scaling and wavelets functions, the lifting scheme decompose that data through three major operations; splitting, prediction and update as shown in Fig. 3.

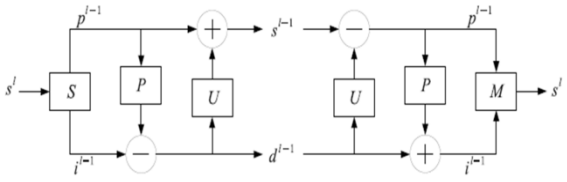

Fig. 3: The Lifting scheme decomposition and reconstruction process.

The power of lifting scheme is that, it starts with very simple wavelet called the lazy wavelet which splits the data onto even and odd sets, then this lazy wavelet is lifted up to produce the desired wavelet and scaling functions by the prediction and the update operations. A simple example of how the prediction and update operators can be used to lift up the lazy wavelet to the Haar wavelet is shown in [16].

The major benefit of using the lifting scheme for surface filtration is that it gives us the ability to decompose and filter complex surface geometries that could not be represented using simple regular data sets.

IV- WAVELETS AND MULTI RESOLUTION ANALYSIS ON SURFACES

Multi-resolution analysis (MRA) for 3D meshes has been an active research area for the past decade. The introduction of the second generation wavelets and lifting scheme [14-17] made the extension of wavelets and MRA possible for all types of 3D meshes and a few algorithms have been proposed [13, 18-22]. The main idea behind MRA is to decompose a high resolution mesh into a lower resolution mesh and details that are needed to recover the original mesh, this operation is repeated iteratively starting from the finest mesh M_∞ and ending wish the coarsest base mesh M_0 as shown in Fig. 4.

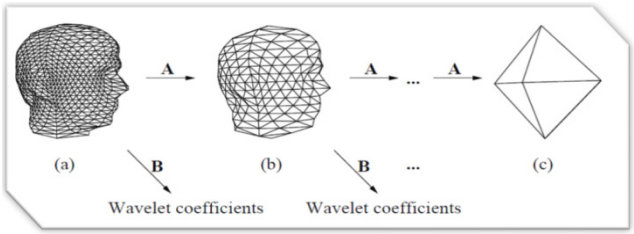

Fig. 4: Decomposition of 3D mesh into approximation and details as proposed by Lounsbery [19].

Lounsbery *et al.* have proposed a bi-orthogonal filter banks to decompose a regular and semi-regular 3D meshes into a lower resolution counterpart and a series of wavelets coefficients as shown in Fig. 4 above. In their method, they made the connection between the nested spaces of scaling functions and 3D mesh decomposition through subdivision. They show that subdivision scheme can be considered to be nested linear spaces required to build the MRA [19]. The decomposition is computed with two analysis filters, A^j and B^j for each resolution level j. The reconstruction is done with two synthesis filters P^j and O^j. They showed that coarser mesh and its wavelet coefficients (V^j and W^j respectively) can be calculated from a finer mesh V^{j+1} using the following equations:

$$V^j = A^j V^{j+1} \quad (1)$$

$$W^j = B^j V^{j+1} \quad (2)$$

The finer mesh V^{j+1} could be recovered from its coarser approximation and wavelets coefficients using a pair of synthesis filters P^j and Q^j;

$$V^{j+1} = P^j V^j + Q^j W^j \quad (3)$$

Where the connection between the analysis and synthesis filters that insures the perfect reconstruction is given by:

$$\begin{bmatrix} A^j \\ B^j \end{bmatrix} = \begin{bmatrix} P^j & Q^j \end{bmatrix}^{-1} \quad (4)$$

This technique works only on regular and semi-regular meshes but fails to handle the irregular cases.

Daubechies *et al.* proposed another technique that can handle an irregular 3D meshes. There technique is based on mesh simplification and subdivision schemes, the authors use a Burt-Adelson pyramid scheme as shown in Fig. 5. The design of the subdivision scheme is carried out by inserting new values in such a manner that the second order differences are minimized [21].

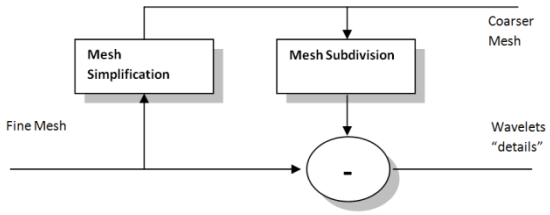

Fig. 5: Decomposition of irregular 3D mesh using Burt-Adelson pyramid-like scheme.

Schroder and Swelden have proposed an extension of the lifting scheme to decompose spherical surfaces [23,24]. In their technique they divide the mesh into two sets of vertices, the first set contains the new vertices resulted from subdivision and the second set contains the old vertices that determine the new values. Then the new vertices are predicted using interpolation techniques.

Bonneau was the first to introduce multi-resolution analysis over non-nested spaces, which are generated by BLac-wavlets which is a combination of the Haar function with the linear B-Spline function. Two major operators were proposed; the smoothing operator to compute the coarse mesh and an error operator to determine the difference between the approximation and the original meshes (Bonneau 1998) [20].

Roy *et al*. have proposed a MRA for irregular meshes based on split and predict operations [22]. This algorithm consists of three main steps: split, predict and down-sampling. The split operator separate the odd and even vertices; the odd vertices are defined as a set of independent vertices which not directly connected by an edge. All the selected odd vertices are to be removed by mesh simplification algorithm in the global down-sampling stage, and then predicted back using the prediction operator that relax the curvature based on the Meyer smoothing operator [25,26]. In fact, the work presented in this paper is inspired by Roy's work and his paper.

Valette *et al.* presented a wavelet-based multi-resolution decomposition of irregular surface meshes. The method is essentially based on Lounsbery decompositions; however the authors introduced a new irregular subdivision scheme. Their algorithm uses a complex simplification technique in order to define surface patches suitable for the irregular [27].

Recently, Szczensa proposed a new multi-resolution analysis for irregular meshes using the lifting scheme, in which she propose a new prediction operator using Voronoi cells in a local neighbourhood [28, 29].

V- FREEFORM SURFACE FILTERING USING THE LIFTING SCHEME

Extending the lifting scheme form 1D and 2D regular cases into 3D irregular meshes is very challenging. In this section, we detail all different blocks required to build the lifting scheme on 3D meshes. The framework of a generalised lifting scheme for 3D meshes is represented in Fig. 6. Fig. 6(a) shows the mesh decomposition stage; an input mesh is decomposed into a coarser mesh (wavelet approximation) and details (wavelet details) by splitting the mesh vertices into two groups; evens and odds. Odd vertices are used to update the even vertices. Even vertices are chosen to rebuild the coarser mesh that approximates the original mesh. The odd vertices, on the other hand, are to be removed. The updated even vertices are used to predict the odd vertices, and then the details coefficients are calculated as the difference between the prediction and the original odd vertices. Fig. 6(b) shows how to reconstruct the original mesh using its approximation and details. All of these different blocks are explained in the following sub-sections.

A. Split operation

The first stage in building the lifting scheme is to split the input data into even and odd. In the case of 1D input; this task is trivial, but for 3D meshes it not straightforward.

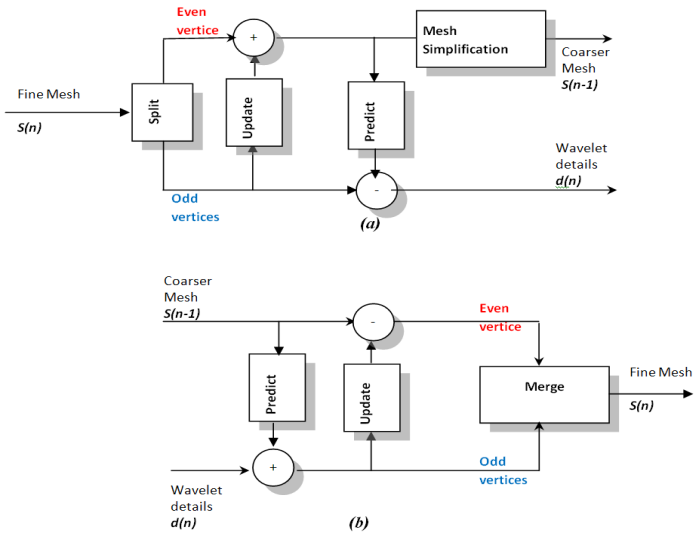

Fig. 6: The Generalised Lifting scheme on 3D meshes. (a) Mesh decomposition. (b) Mesh reconstruction

One important notice in the 1D case is that each odd index is surrounded by even indices. This observation is kept true in our proposed algorithm and so all odd vertices have to be surrounded by even vertices and no two odd vertices can share an edge. On the other hand, even vertices can be adjacent to each other and form edges in the mesh. The output of the split operator can be mathematically described as:

$$S(M^j) = \begin{cases} {v_{odd}}^j \\ N({v_{odd}}^j) \end{cases} \quad (5)$$

Where;

M^j represents an input mesh at level j. ${v_{odd}}^j$ is the set of odd vertices at level j and $N({v_{odd}}^j)$ is the set of the even vertices that represent one-ring neighbourhood of the odd vertices.

Different methods can be used to select the odd vertices, and the quality of the output coarser mesh depends entirely on the selected odd vertices. So, better selection algorithm will produce better approximation. Three different split operators are implemented and discussed on this paper; random, shortest-edges and quadric error metric (QEM) split operators.

- Random split operator:

In random split, an initial vertex is selected to be odd randomly and then all its neighbours are set to be even, then a new unprocessed vertex is selected to be odd and all of the neighbours are even. This process ends when no more vertices can be selected.

- Shortest-edges split operator:

The second split operator is based on the shortest edges in the mesh. Initially, the length of all edges are calculated and then sorted in ascending order in a list. One vertex of the shortest edge is selected to be odd and all the adjacent vertices are

locked to be even. Then, the second shortest edge is selected and if one of its vertices are not processed yet, (neither even nor odd), then that vertex is selected to be odd and all adjacent to be even and so on. The algorithm continues until all edges have been processed.

- Quadric error Metric (QEM) split operator:

The third splitting algorithm is based on the quadric error metrics which is originally proposed by Garland and Hechbert [30] to simplify triangle meshes with high accuracy. The algorithm uses iterative vertex pair contraction to simplify a surface and maintain a geometric error approximation of the triangular meshes using the quadric matrices. These vertex pairs are used to identify the odd vertices in our splitting module.

Vertex-pair contraction is carried out iteratively based on the cost of the contraction. Small costs contractions are performed first keeping higher costs to the end. We summarise the algorithm of calculating the cost of the contraction using the following steps. Readers are referred to Garland paper [30] for more details.

1- For each vertex in the mesh, calculate the error quadric (Q) matrix using the following equation:

$$Q(v) = \sum_{p \epsilon\, faces(v)} \mathrm{K_p} \tag{6}$$

where;

$$\mathrm{K_p} = \begin{bmatrix} a^2 & ab & ac & ad \\ ab & b^2 & bc & bd \\ ac & bc & c^2 & cd \\ ad & bd & cd & d^2 \end{bmatrix} \tag{7}$$

and;

- *[a b c d]* represents the plane defined by the equation $ax + by + cz + d = 0$ where $a^2 + b^2 + c^2 = 1$.
- *faces(v)* are the set of faces that share the vertex *v*. Each face of these faces is part of the plane defined by the coefficients *[a b c d]*.

2- For each edge e_{ij} or (v_i-->v_j) in the mesh calculate the contraction cost by:

$$E(e_{ij}) = min \begin{cases} v_i \ .(Q_i + Q_j).{v_i}^T \\ v_j \ .(Q_i + Q_j){v_j}^T \end{cases} \tag{8}$$

where;
$E(e_{ij})$ is the cost of contracting the edge e_{ij}, ${v_i}^T$ is the transpose of v_i and $v_i = [x\ y\ z\ 1]$. Note that if the cost using the vertex v_i is less than the cost obtained by using v_j then v_i is an even vertex and $v_j$is an odd vertex that has to be removed.

3- Sort the edges according to their costs, and start selecting the odd vertices based on the criteria described in step 2.

Similar to the shortest-edges method, this method not only selects the odd vertices but also it chooses the even partners that will be needed in mesh simplification algorithms as will be described later in the paper.

B. Prediction operator

The design of the prediction operator plays a key role in surface filtrating using the lifting scheme. It has to predict the properties of the odd vertices using the even vertices. In our application, these properties could be the vertex's position or the vertex texture, the residual normal distance between the nominal and the measured surfaces at that vertex.

In the split operator, odd vertices are chosen so that each odd vertex is surrounded by even neighbours. Therefore, the prediction operator depends on the even-ring neighbourhood of the odd vertex.

Traditionally, the predicted odd value is a weighted summation of the values of its even neighbours. Many algorithms have been proposed to design these weights and cubic spline prediction operator is one of the famous methods to calculate these weights in traditional lifting scheme.

In triangular meshes, the predicted odd value is calculated using one-ring even neighbours by the equation:

$$f(v_i) = \sum_{j \epsilon\, N(v_i)} \omega_{i,j} \ . f(v_j) \tag{9}$$

Where $f(v_i)$ could be any function or attribute defined over the vertex v_i, this function in our application is the surface texture.

If the filtration is carried out on the mesh vertices themselves and not on a function defined over that mesh, then position of the vertex is to be predicted and the predicted location of an odd vertex is give by:

$$\left.\begin{aligned} y_i &= \sum_{j \epsilon\, N(v_i)} \omega_{i,j} \ . y_j \\ y_i &= \sum_{j \epsilon\, N(v_i)} \omega_{i,j} \ . y_j \\ z_i &= \sum_{j \epsilon\, N(v_i)} \omega_{i,j} \ . z_j \end{aligned}\right\} \tag{10}$$

Where $\omega_{i,j}$ are the weights of the even vertices in the even-ring $N(v_i)$.

Designing the weights is very important and different weights can significantly improve the filtration process. These

weights could be calculated using different methods depending on the application. The simplest algorithm to calculate these weights is by using equal weights for all the surrounding neighbours.

$$\omega_{i,j} = \frac{1}{NN} \tag{11}$$

where; NN is the number of even neighbours in the even-ring neighbourhood.

In this paper, the author adopted the weights calculated using the curvature-relaxing operator as proposed by Roy *et al.* [22] and which is given by:

$$\omega_{i,j} = \frac{\cot \alpha_{i,j} + \cot \beta_{i,j}}{\sum_{l \in even\_ring} \cot \alpha_{i,l} + \cot \beta_{i,l}} \tag{12}$$

where; $\alpha_{i,j}$ and $\beta_{i,j}$ are the angles opposite to the edge $e_{i,j}$ as shown in the Fig. 7.

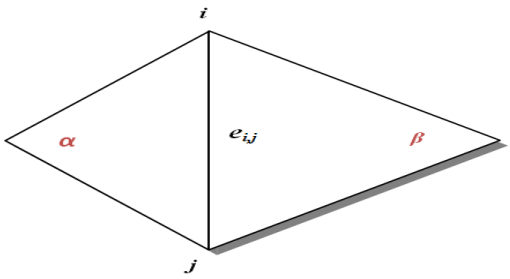

Fig. 7: The definition of relaxation angles α and β for the edge ei,j .

C. Update operator

Traditionally, the update operator preserves some features from the input higher resolution signal to the output lower resolution coarse signal. For example, the update operator for designing a Haar transform using the lifting scheme insures that the average of the input fine signal is equal to the average of the output coarse signal. Based on the previous observation, the update operator in the 3D mesh case has also to preserve some important features in all approximated meshes at all different decomposition levels.

In this paper, we choose to preserve the average value of the vertex-ring before and after removing the odd vertex, thus the update is given by:

$$U[(f(v_{even})] = \frac{NN.(f(v_{odd}) - \sum_{j \in N(v_{odd})}(f(v_j))}{NN \times (NN+1)} + f(v_{even}) \tag{13}$$

where;

NN is the number of even neighbours in the even ring neighbourhood.

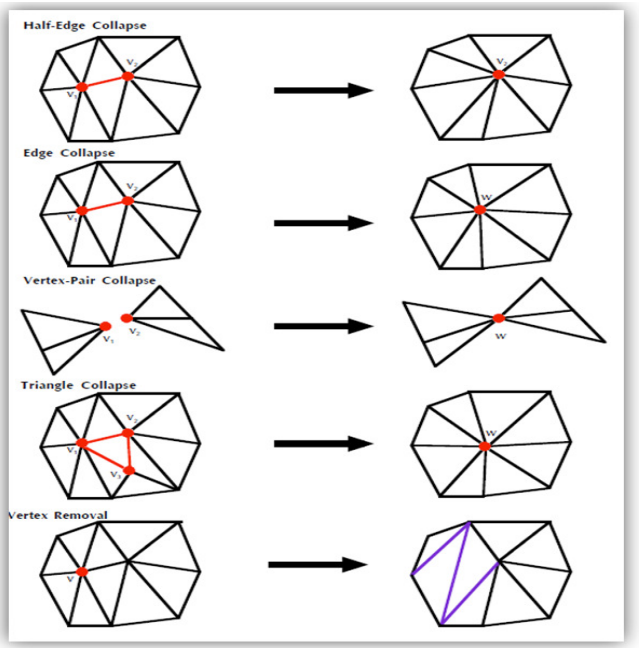

Fig. 8: Different mesh simplifications algorithms

D. Mesh simplification (The approximation)

Mesh simplification or down-sampling is the process of reducing the number of faces, edges and vertices while attempting to preserve the overall geometry, shape, boundaries as much as possible. It is the step that produces the approximated coarser meshes (wavelet approximations), which can be used as an input for further decomposition levels.

Many algorithms have been proposed for mesh simplification as shown in Fig. 8. These algorithms can be roughly divided into three major groups; the first group simplify the mesh by selecting an edge to be collapsed, the second define a face to be removed and the third type relies on selecting vertex to be removed, as shown in the figure. The half-edge collapse does not introduce a new vertex position but rather it simplifies (subsample) the mesh using the same vertices locations, hence, half-edge collapse is adopted to perform the simplification step in implementing of the lifting scheme over 3D meshes.

E. The details

The details coefficients is defined as the Euclidean distant or a vector between the odd vertex properties and its prediction. These coefficients must have all the information needed to perform a perfect reconstruction of the original mesh.

In the proposed algorithm the details are stored as number of records, the number of details records is equal to number of odd vertices selected by the split operator. Each record preserves all the information that is required for the reconstruction, these information includes; the details vectors and all the edges and topological information before removing that odd vertex.

F. Merge Operator

The merge operator, mesh up-sampling, defines how to re-insert new vertices into the mesh. The insertion of new vertex into the mesh is controlled by the details record of that vertex. The mesh topology before removing the odd vertex must be preserved and perfectly reconstructed by the merge operator. In this paper, the merge operator was carried out using the vertex-split algorithm adopted from the Progressive Mesh (PM) procedure [31].

VI- Results and Discussions

The proposed lifting scheme has been implemented and tested to filter measured and simulated surfaces represented by 3D irregular triangular meshes and the results are shown and discussed in this section.

Firstly, the proposed algorithm has been demonstrated by decomposing and reconstructing a simple 2D mesh shown in Fig. 9. The original 2D mesh is shown in Fig. 9(a). In this experiment only one odd vertex has been selected by the split operator, which is vertex 6 in the middle of the figure this odd vertex has to be removed to produce a simplified coarser mesh.

To remove the odd vertex, the algorithm has to chose one edge to be collapsed, the edge $e(6\text{-}8)$ is chosen in our example. Performing half-edge collapse on the edge $e(6,8)$ requires removing the vertex 6 and all edges that have the vertex 6 as an end vertex, and then to reconnect those edges to vertex 8 instead. Fig. 9(b) shows the coarser mesh.

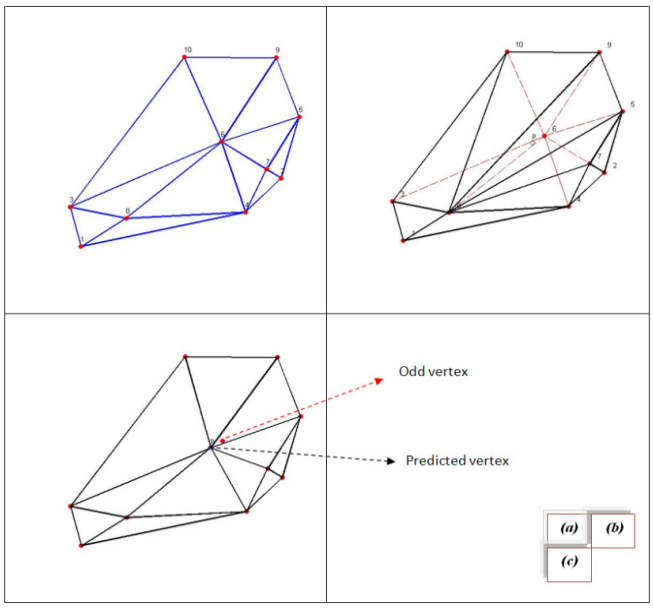

Fig. 9: Demonstration of the lifting scheme on 2D mesh. (a) The original mesh ((10 vertices, 11 faces and 20 edges)). (b) The mesh after collapsing the edge e(6-8) ((9 vertices, 9 faces and 17 edges)). (c) The constructed mesh using the vertex-split and also using a prediction vertex p calculating using the even-ring.

The even-ring neighbours, vertices (10, 9, 5, 7, 4, 8 and 3) in our example, are used to predict the odd vertex. The predicted vertex is shown as the vertex p in Fig. 9(b). As shown in figures 9(b) and (c), the predicted vertex is very close to the original odd vertex, vertex 6 in our example, and therefore the predicted vertex could be used to construct the mesh as shown in Fig. 9(c). In this experiment, the prediction operation is carried out using the equal-weights prediction operation discussed earlier in this paper.

The constructed mesh must have exactly same topology as the original mesh; the new vertex p is inserted into the coarse mesh in (b) while preserving the relation between the odd vertex and its even-ring as shown in Fig. 9(c).

The next step is to test the algorithm to filter real and simulated surfaces. Fig. 10 shows the filtration framework that has been used to filter our surfaces. As shown in the figure, the input surface mesh is decomposed into N-Levels, and the details coefficients are filtered out and set to zero before the surface is reconstructed again. More decomposition levels mean a smoother output surface. However, the number of decomposition levels is limited and no further decomposition is possible once we reach the base mesh that could not be simplified anymore. Therefore, more filtration could be achieved by reapply the output filtered surface as an input to the filtration system and repeat the process as many times as needed, which is represented by the M-iterations in Fig. 10.

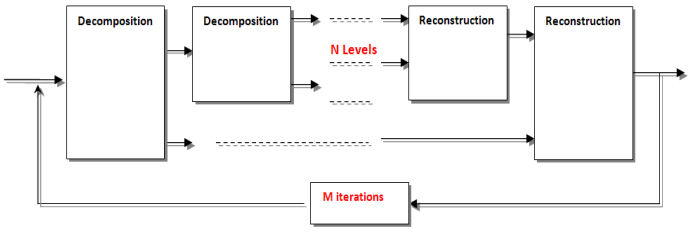

Fig. 10: Surface filtration algorithm using the lifting scheme.

A. Simulated surfaces

Four computer generated surfaces are used to test the performance of the proposed algorithm. These surfaces are designed to cover a wide range of freeform surfaces with different topological types. The first surface is a saddle shaped surface which is a typical example of non-Euclidean surface with negative curvature. The second surface is a sphere that represents positive curvature non-Euclidean geometry. The third and forth surfaces are more complicated surfaces with non-constant curvatures. We refer to the third and fourth surfaces as bumpy and wavy surfaces respectively. All of these surfaces are shown in Fig. 11.

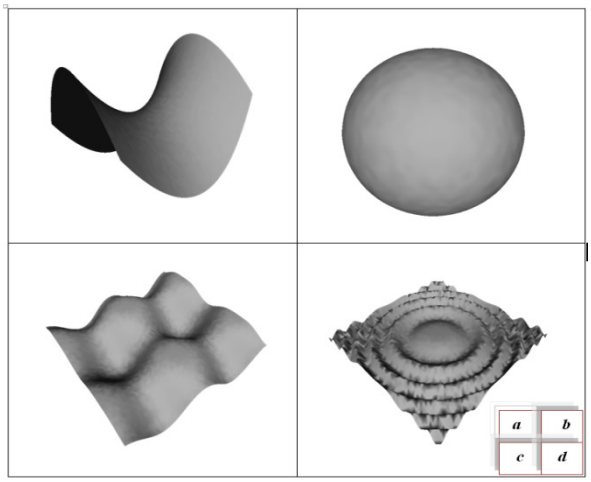

Fig. 11: Computer generated surfaces; (a) non-Euclidean negative curvature surface "saddle shaped surface" (b) positive curvature surface "sphere", (c) and (d) non-constant curvature surfaces represented by bumpy and wavy surfaces respectively

An artificial Gaussian noise is add to these surfaces to represent the texture that needed to be filtered out using the proposed lifting scheme and the filtration results are shown in figures 12-15.

Fig. 12 shows the results of applying the proposed algorithm on the saddle shaped surface. The original noisy surface is show in Fig. 12(a). Figures 12 (b) – (f) show the results using 1, 4, 8, 16 and 24 decomposition levels respectively. Figures 12 (g) – (i) on the hand, show the results of using 24 decomposition levels and 2, 3 and 4 iterations respectively.

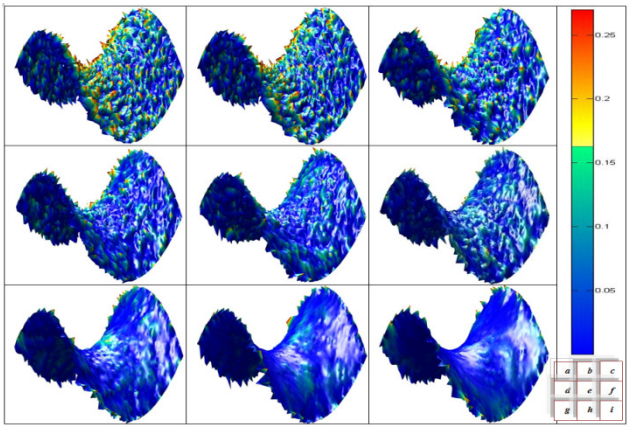

Fig. 12: Texture filtration results of the saddle shaped surface; (a) the original textured surface. (b)- (f) the filtration results using 1, 4, 8, 16 and 24 decomposition levels respectively. (g)- (i) The filtration results using 24 decomposition levels and 2, 3 and 4 iterations respectively.

The proposed algorithm has been also applied to filter the other surfaces and the results are shown in figures 13, 14 and 15 for the sphere, bumpy and wavy surfaces respectively.

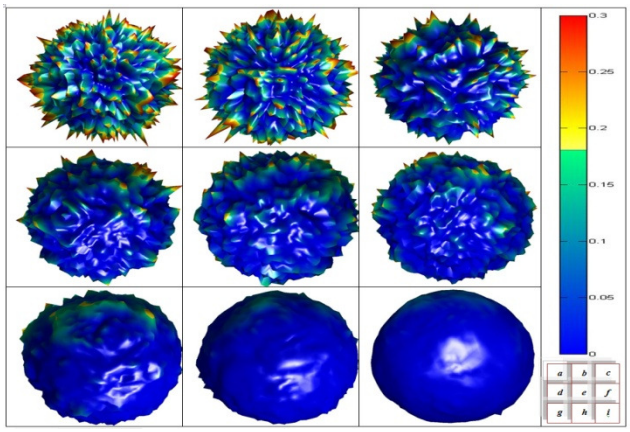

Fig. 13: Texture filtration results of the spherical surface; (a) the original textured surface. (b)- (f) the filtration results using 1, 4, 8, 16 and 24 decomposition levels respectively. (g)- (i) The filtration results using 24 decomposition levels and 2, 3 and 4 iterations respectively.

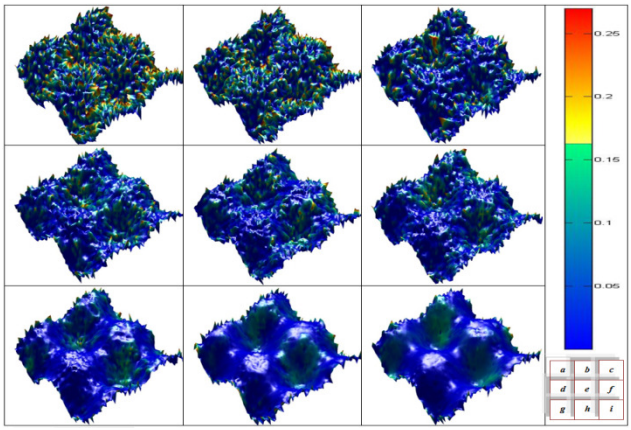

Fig. 14: Texture filtration results of the bumpy surface; (a) the original textured surface. (b)- (f) the filtration results using 1, 4, 8, 16 and 24 decomposition levels respectively. (g)- (i) The filtration results using 24 decomposition levels and 2, 3 and 4 iterations respectively.

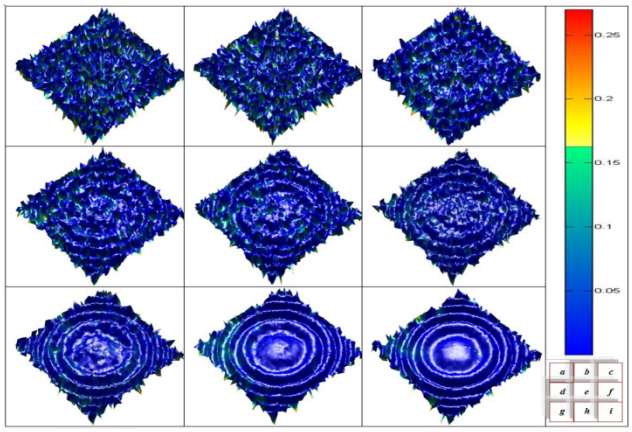

Fig. 15: Texture filtration results of the wavy surface; (a) the original textured surface. (b)- (f) the filtration results using 1, 4, 8, 16 and 24 decomposition levels respectively. (g)- (i) The filtration results using 24 decomposition levels and 2, 3 and 4 iterations respectively.

Figures 16 and 17 show the output of the mesh simplification or mesh down-sampling operation using the half-edge collapse algorithm as discussed earlier in the paper. In these figures the coarser meshes (wavelet approximations) after 1, 4, 8, 16 and 24 decomposition levels, for the saddle and sphere surfaces, are shown in figures (a)-(f) respectively.

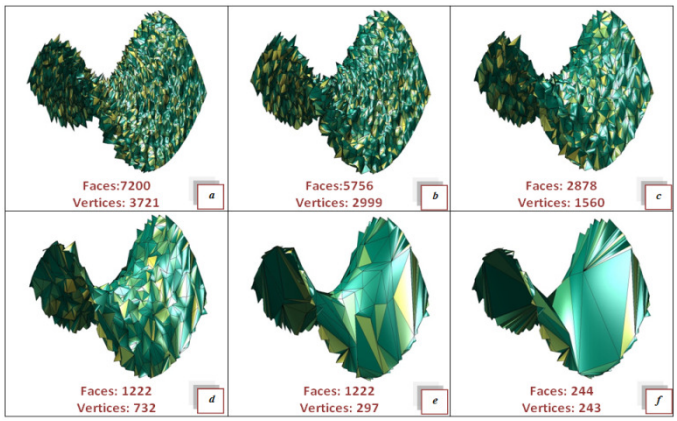

Fig. 16: The approximated output meshes (wavelet approximations) for the saddle-shaped surface at different decomposition levels. (a) The original finest input mesh, (b)-(f) the approximated coarse mesh after 1, 4, 8, 16 and 24 decomposition levels respectively.

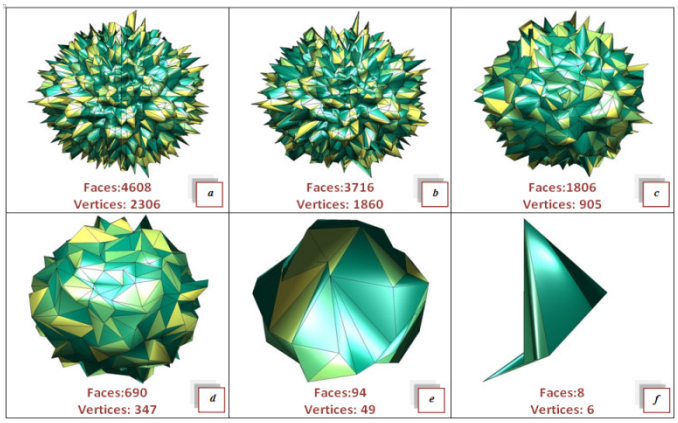

Fig. 17: The approximated output meshes (wavelet approximations) for the spherical surface at different decomposition levels. (a) The original finest input mesh, (b)-(f) the approximated coarse mesh after 1, 4, 8, 16 and 24 decomposition levels respectively.

Fig. 18 shows the output of the split operator using the QEM algorithm as explained above. The figure demonstrates how the odd and even vertices are distributed and number of even and odd vertices are shown at the first, second, firth, eighth, sixteenth and twenty-forth level of the decomposition. The odd vertices are represented by blue dots while the even vertices are the red dots in the figure. In this paper, we did not allow any boundary vertex to be an odd vertex, this will insures that all odd vertices have a complete ring of neighbourhood and thus will produce more accurate prediction and improves the filtration process and also eliminates the boundary problem that will occur when predicting at the boundary.

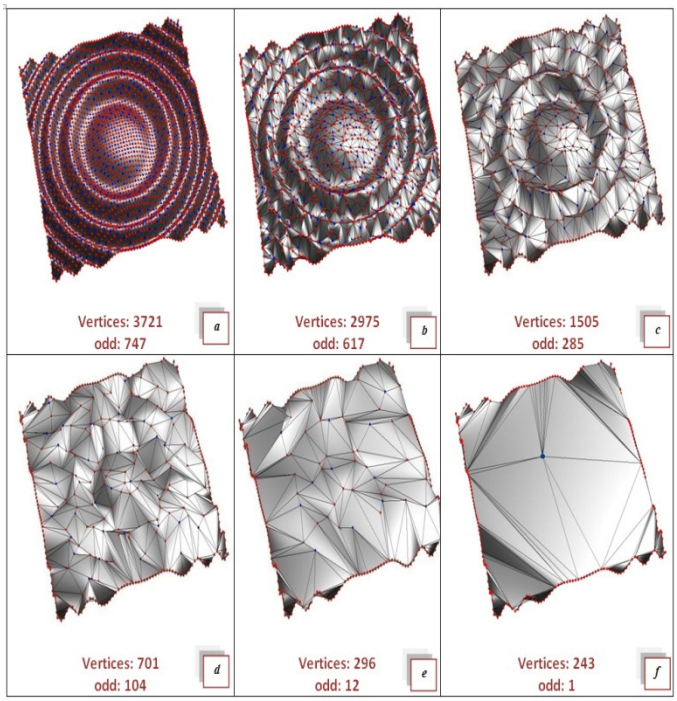

Fig. 18: A demonstration of the split operator using the QEM algorithm on the wavy surface. The distribution of odd vertices at the first, second, fourth, eighth, sixteenth and twenty-fourth are shown in (a)-(f) respectively. Boundary vertices are not allowed to be odd vertices.

Fig. 19 compares between the three different split operators discussed earlier in the paper, i.e.; the random, shortest-edges and QEM algorithms. Fig. 19 (a) shows the percentage of odd vertices at different decomposition levels for the saddle shape surface, while Fig. (b) shows the same but for the wavy surface. Both figures show that the random and the shortest-edges give higher odd vertices percentage in the first decomposition levels but quickly drop and give very low percentage at higher levels. On the other hand, the QEM has the smallest percentage in the beginning but it slow decay and cover more decomposition levels. This means that the QEM split operator gives the best mesh approximation output and the mesh gradually become coarser at each decomposition level as shown in Fig. 16 and 17.

B. measured surfaces

After the initial application of the proposed algorithm to computer generated surfaces, the lifting scheme filtering was performed on real surface measurement data. The data were obtained from coordinate measuring machine (CMM) measurement of portion of hip replacement components. These two measured surfaces are shown in Fig. 20; we refer to these two surfaces as hip-part1 and hip-part2 as shown in Fig. 20(a) and (b) respectively. As with the computer generated surfaces an extra artificial Gaussian noise is added to these surfaces and then these surfaces are filtrated using the proposed algorithm.

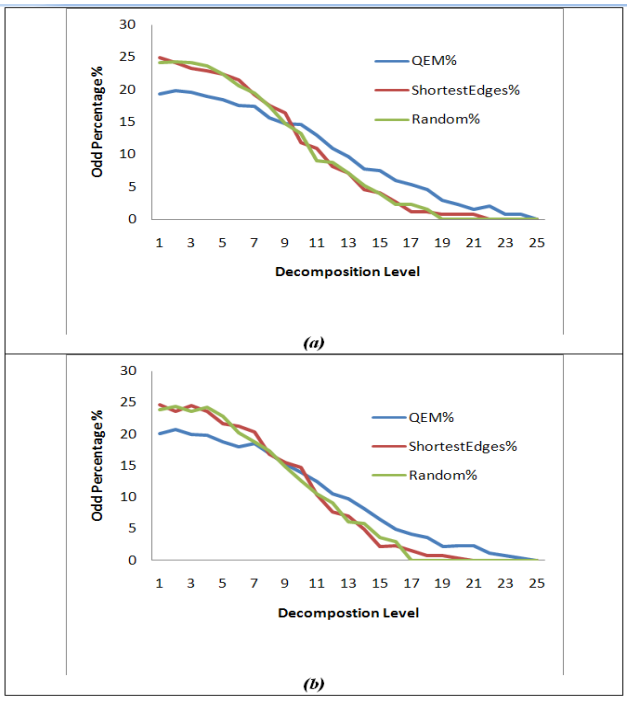

Fig. 19: Comparison between the random, shortest-edges and the QEM split operators at different decomposition levels; (a) the results of saddle-shaped surface, (b) the results of the wavy surface.

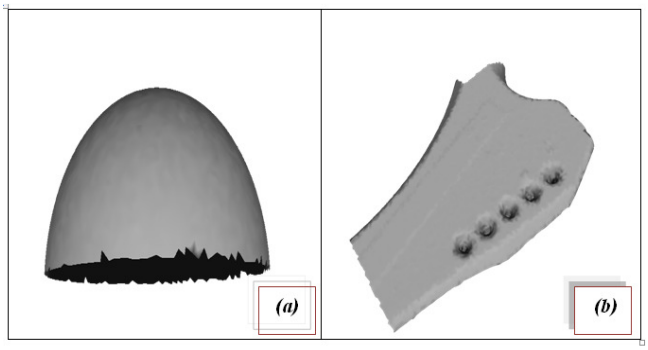

Fig. 20: Two real measured surfaces obtained with CMM for hip replacement component. We refer to these surface as; (a) hip-part1 and (b) hip-part2.

Figures 21-22 show the results of applying the proposed lifting technique to filter the surface texture at different decomposition levels and iterations. As with the simulated results, the proposed algorithm was successfully capable of smoothing the texture to different scales according to the decomposition levels and number of iterations. Figures 23-24 show the outputs of the mesh-simplification process (wavelet approximations) at different decomposition levels for the two surfaces shown in Fig. 20.

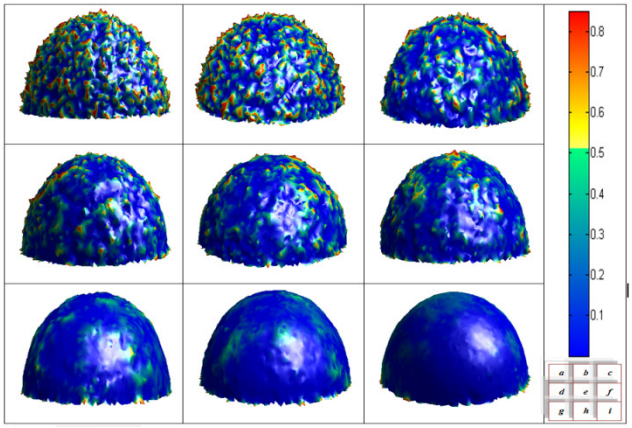

Fig. 21: Texture filtration results of the hip-part1 surface; (a) the original textured surface. (b)- (f) the filtration results using 1, 4, 8, 16 and 24 decomposition levels respectively. (g)- (i) The filtration results using 24 decomposition levels and 2, 3 and 4 iterations respectively.

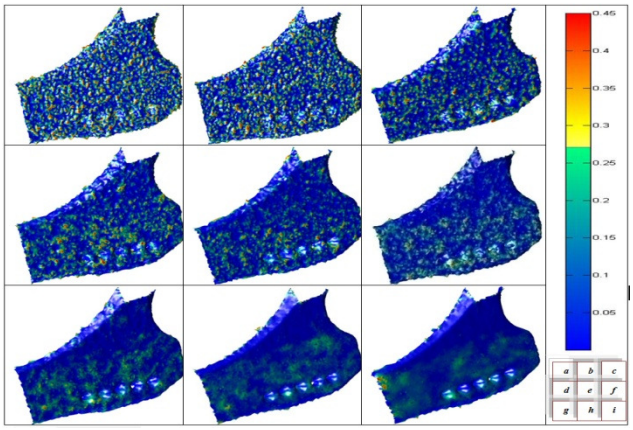

Fig. 22: Texture filtration results of the hip-part2 surface; (a) the original textured surface. (b)- (f) the filtration results using 1, 4, 8, 16 and 24 decomposition levels respectively. (g)- (i) The filtration results using 24 decomposition levels and 2, 3 and 4 iterations respectively.

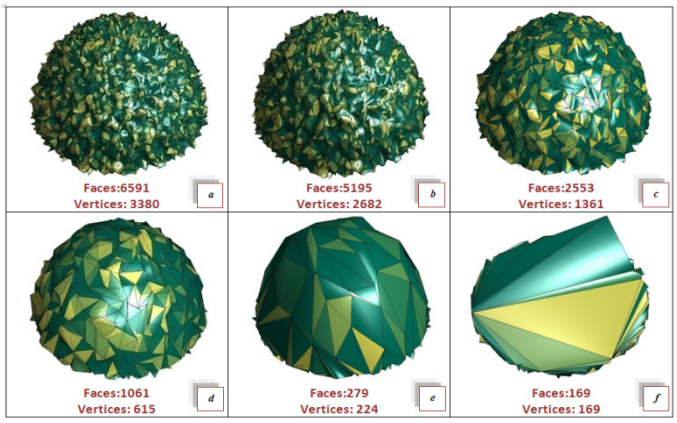

Fig. 23: The approximated output meshes (wavelet approximations) for the hip-part1 surface at different decomposition levels. (a) The original finest input mesh, (b)-(f) the approximated coarse mesh after 1, 4, 8, 16 and 24 decomposition levels respectively.

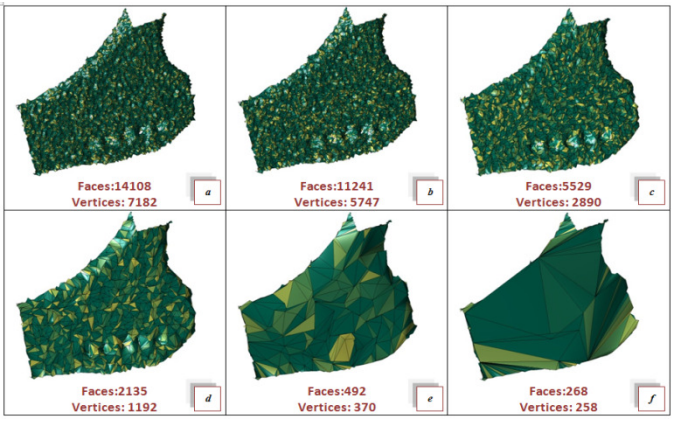

Fig. 24: The approximated output meshes (wavelet approximations) for the hip-part2 surface at different decomposition levels. (a) The original finest input mesh, (b)-(f) the approximated coarse mesh after 1, 4, 8, 16 and 24 decomposition levels respectively.

VII- CONCLUSIONS

In this paper, a generalised lifting scheme to filter the texture of freeform surfaces represented by 3D irregular triangular meshes has been proposed. The proposed algorithm has been applied to filter the texture of computer generated and real measured free-from surfaces. The results show that the proposed lifting algorithm is robust and has good potential for free-from surface filtration. Furthermore, the proposed algorithm is capable to filter the surface texture at different scales depending on the decomposition levels and the number of iterations.

Moreover, three split operators have been implemented; the random, the shortest-edges and the quadric error metric (QEM) methods. The QEM algorithm gives the best surface approximation of the original surface after the simplification process. However, the random and shortest-edges give higher number of odd vertices at lower decomposition levels as shown in the paper.

The prediction operator plays an important role in the filtration process. In this paper, two prediction methods were discussed, the first is using equal weights, and the second is using weights that would minimize the curvature. The choice of the weights depends on the surface being filtered, therefore, more prediction methods need to be investigated to cover a wide range of freeform surfaces.

REFERENCES

[1] Abbott, E.J. & Firestone, F.A. 1933 Specifying surface quality: a method based on accurate measurement and comparison. Mechanical Engineering 55: 569–572.

[2] Greenwood, J. A. 1984 A unified theory of surface roughness. *Proc. R. Soc. A***393**, 133–157. (doi:10.1098/rspa.1984.0050)

[3] Jiang, X., Scott, P. J., Whitehouse, D. J. & Blunt, L. 2007a Paradigm Shifts in surface metrology. Part I, Historical philosophy. *Proc. R. Soc. A* **463**, 2049–2070. (doi:10.1098/rspa.2007.1874)

[4] Jiang, X., Scott, P. J., Whitehouse, D. J. & Blunt, L. 2007b Paradigm Shifts in surface metrology. Part II, The current shift. *Proc. R. Soc. A* **463**, 2071–2099. (doi:10.1098/rspa.2007.1873)

[5] Whitehouse, D. 2002 Surfaces and their Measurement. *Hermes Penton Ltd.*

[6] ISO 11562: 1996 Geometric product specification (GPS) Surface Texture: profile method metrological characteristics of phase correct filters.

[7] ISO/FDIS 16610-21: 2010 Geometrical product specifications (GPS) - Filtration - Part 21: Linear profile filters: Gaussian filters

[8] ISO/CD 16610-61: 2010 Geometrical product specifications (GPS) - Filtration - Part 61: Linear areal filters: Gaussian Filters

[9] ISO/TS 16610-31: 2010 Geometrical Product Specification (GPS) - Filtration.

[10] ISO/FDIS 25178-2: 2010, Geometrical Product Specification (GPS) - Surface Texture: Areal - Part 2: Terms, definitions and surface texture parameters.

[11] Jiang, X., Cooper, P. & Scott, P. J., 2011 Freeform surface filtering using the diffusion equation. *Proc R. Soc A*, Vol. **467**, Issue. **2127**, pp. 841–859. (DOI: 10.1098/rspa.2010.0307).

[12] Hubeli, A. & Gross, M. 2000 A survey of surface representations for geometric modelling. *Technical Report 335, ETH Zurich, Computer Science Department.*

[13] Guskov, I., Sweldens, W. & Schroder, P. 1999 Multiresolution signal processing for meshes. *Proceedings of ACM SIGGRAPH*, pp. 325–334.

[14] Sweldens, W. 1995 The Lifting Scheme: A New Philosophy in Biorthogonal Wavelets Reconstructions. *Wavelet applications in signal and image processing III*, pp. 68-79.

[15] Sweldens, W. 1996a Wavelets and Lifting Scheme: A 5 minutes tour. Z. Angew. Math. Mec , 76, pp. 41-44.

[16] Sweldens, W. 1996b "Wavelets and the Lifting Scheme: A 5 Minute Tour. *Z. Angew. Math. Mech* vol. **76**, no. **2**, pp. 4-7.

[17] Sweldens, W. 1998 The lifting scheme: A construction of second generation wavelets. SIAM Journal on Mathematical Analysis, vol. 29, no. 2, pp. 511-546.

[18] Eck, M., DeRose, T., Duchamp, T., Hoppe, H., Lounsbery, M. & Stuetzle, W. 1995 Multiresolution Analysis of Arbitrary Meshes. In *SIGGRAPH 95 Conference Proceedings*, *ACM SIGGRAPH, Addison Wesley, Reading, MA*, pp. 173–182.

[19] Lounsbery, M., DeRose, T. & Warren, J. 1997 Multi-resolution Analysis for Surfaces of Arbitrary Topological Type. *ACM Transactions on Graphics*, Vol. **16**, No, **1**, pp. 34-73.

[20] Bonneau, G. P. 1998 Multiresolution analysis on irregular surface meshes. *IEEE Transactions on Visualization and Computer Graphics* vol. **4**(4), pp. 365–378.

[21] Daubechies, I., Guskov, I., Schroder, P. & Sweldens, W. 1999 Wavelets on Irregular Point Sets. *Phil. Trans. R. Soc. Lond. A*, **357**, pp.2387-2413.

[22] Roy, M., Foufou, S., Koschan, A., Truchetet, F. & Abidi, M. 2005 Multiresolution Analysis for Meshes with Appearace Attributes. *Proc. IEEE on Image Processing ICIP2005*, vol. **III**, pp. 816-819.

[23] Schroder, P. & Sweldens, W. 1995a Spherical Wavelets: Texture Processing. *In P. Hanrahan and W. Purgathofer, editors, Rendering Techniques 95, Springer Verlag, New York, August*.

[24] Schroder, P. & Sweldens, W. 1995b Spherical Wavelets: Efficiently Representing Functions on the Sphere". In *EGRW 95*, pp. 252–263.

[25] Desbrun, M., Meyer, M., Schr¨oder, P., & Barr, A., 1999 Implicit fairing of irregular meshes using diffusion and curvature flow. *Proceedings of ACM SIGGRAPH*, pp. 317–324.

[26] Meyer, M., Desbrun, M., Schr¨oder, P., & Barr, A. 2002 Discrete differential-geometry operators for triangulated 2-manifolds. *Proceedings of Visualization and Mathematics*.

[27] Valette, S. & Prost, R. 2004 Wavelet-based multiresolution analysis of irregular surface meshes. *IEEE Transactions on Visualization and Computer Graphics,* vol. **10**, no. 2, pp. 113–122.

[28] Szczesna, A. 2007 The multiresolution analysis of triangle surface meshes with lifting scheme. in *Proceedings of MIRAGE Conference on Computer Vision/Computer Graphics Collaboration Techniques*.

[29] Szczesna, A. 2008 Designing lifting scheme for second generation wavelet-based multiresolution processing of irregular surface meshes. *Proceedings of Computer Graphics and Visualization*.

[30] Garland, M. & Heckbert, P. 1997 Surface simplification using quadric error metrics. *Proceedings of ACM SIGGRAPH*, 209–216.

[31] Hoppe, H. 1996 Progressive meshes. *Proceedings of the 23rd annual conference on Computer graphics and interactive techniques SIGGRAPH* **9630**, pp. 99-108.